

<https://doi.org/10.48047/AFJBS.6.2.2024.4675-4711>



African Journal of Biological Sciences

Journal homepage: <http://www.afjbs.com>



Research Paper

Open Access

PHYTOCHEMICAL PROFILING AND SOIL INTERACTIONS OF CURCUMA CAESIA ROXB FROM NORTHEAST INDIA: A HOLISTIC APPROACH TO MEDICINAL POTENTIAL

RANA MUKHERJEE ^A, DEBOJA SHARMA ^{B*}, ANKITA KALITA ^C,
SUBHADEEP SARKAR ^D, GAURI DUTT SHARMA ^E

*CORRESPONDING AUTHOR: DR. DEBOJA SHARMA,

^{A, B, C, D, E} UNIVERSITY OF SCIENCE AND TECHNOLOGY MEGHALAYA, RI-
BHOI, MEGHALAYA,
PIN CODE:793101, INDIA.

Abstract

Curcuma caesia Roxb. (Black Turmeric), a medicinal plant native to Northeast India, was investigated for its phytochemical composition and therapeutic potential. This study, conducted in August 2022 across four regions of Northeast India (Nongpoh, Meghalaya; Khetri and Karbianglong, Assam; and Moirang, Manipur), aimed to assess the phytochemical profile and examine the influence of soil characteristics on bioactive compound synthesis. Rhizome samples were analyzed using Soxhlet extraction, Fourier-Transform Infrared Spectroscopy (FTIR), Gas Chromatography-Mass Spectrometry (GC-MS), and Liquid Chromatography-Mass Spectrometry (LC-MS). Quantitative estimation of curcumin content and Principal Coordinate Analysis (PCoA) were also performed. GC-MS identified 18 compounds including Linalool, Camphor, and Benzofuran, while LC-MS revealed 9 compounds such as 2,3-Dehydrokieveitone and Pyropheophorbide a. FTIR analysis indicated the presence of eight functional groups. Moirang samples showed the highest curcumin content (0.0117 g). Phytochemical screening confirmed the presence of reducing sugars, alkaloids, flavonoids, steroids, and tannins. Soil analysis demonstrated that acidic soils with high organic matter were associated with higher curcumin and phenolic content. PCoA revealed distinct clustering patterns based on regional differences. These findings highlight the pharmaceutical significance of *C. caesia* and the role of soil properties in enhancing its bioactive potential. The integration of phytochemistry and soil science provides a foundation for optimizing the cultivation and medicinal applications of this valuable plant.

Keywords: Black turmeric, *Curcuma caesia* Roxb, Soil characteristics, Phytochemical composition, Bioactivity, Northeast India, Medicinal plants.

Volume 6, Issue 2, Feb 2024

Received: 05 Jan 2024

Accepted: 03 Feb 2024

Published: 25 Feb 2024

[doi:10.48047/AFJBS.6.2.2024.4675-4711](https://doi.org/10.48047/AFJBS.6.2.2024.4675-4711)

Introduction:

Curcuma caesia Roxb., commonly known as black turmeric, is an endangered perennial herb native to India and Southeast Asia. Almost all parts of this plant possess medicinal properties, giving it high economic importance. This research focuses on its bluish-black rhizomes, which hold significant medicinal potential. Traditionally used in Southeast Asia to treat ailments such as asthma, tumors, and skin disorders, its therapeutic properties are attributed to its high curcumin content and diverse bioactive compounds. Recent pharmacological studies have identified bioactive components, such as camphor, ar-curcumin, and borneol, as promising candidates for drug development (**Paudel et al., 2024**).

The *Curcuma* genus is well-documented for its diversity of bioactive compounds, including curcuminoids, phenolics, terpenoids, and essential oils. While *C. longa* (turmeric) is widely recognized for its curcumin, the potential of *C. caesia* remains largely underexplored by the research community (**Dosoky & Setzer, 2018; Paudel et al., 2024; Rahaman et al., 2020**). Traditionally, the rhizomes of *C. caesia* have been used to heal wounds, address digestive issues, and provide antimicrobial and anti-inflammatory relief, making it an integral part of South Asian healthcare practices (**Raj et al., 2018**). According to **Pebam et al. (2022)**, the phytochemicals in Indian medicinal plants like *C. longa* and *C. caesia* are heavily influenced by regional soil characteristics, which impact their therapeutic efficacy. These compounds exhibit significant pharmacological properties, such as antioxidant, anti-inflammatory, anticancer, and antimicrobial activities (**Devi et al., 2015; Elhawary et al., 2024**).

Despite its traditional significance and preliminary scientific studies, the full therapeutic potential of *C. caesia* remains untapped, with many bioactive compounds yet to be thoroughly investigated for clinical applications (**Paudel et al., 2024**). While some excellent foundational research exists, such as the study by **Devi and Mazumder (2016)**, which demonstrated that methanolic extracts of *C. caesia* **Roxb.** exhibit protective effects against cyclophosphamide-induced genotoxicity and oxidative stress by scavenging free radicals like ABTS (2,2'-azino-bis (3-ethylbenzothiazoline-6-sulphonic acid)), there is a notable lack of research addressing the environmental conditions that facilitate the growth of this endemic plant in Northeastern Indian regions.

To address this gap, this study employs advanced analytical techniques—Fourier-Transform Infrared Spectroscopy (FTIR), Gas Chromatography-Mass Spectrometry (GC-MS), and Liquid Chromatography-Mass Spectrometry (LC-MS)—to first identify and characterize the bioactive compounds in *C. caesia* collected from four regions in Northeast India. Then soil samples from these four locations were analysed for their pH, organic carbon, and other nutrient content, allowing us to draw insights into the phytochemical profile of *C. caesia*. Traditionally acidic soils rich in organic matter are believed to be good promoters of phenolic compounds and flavonoids, essential contributors to the therapeutic effectiveness of *C. caesia* (**Paudel et al., 2024**).

Recognizing this, the study investigates how soil and climatic conditions influence the plant's medicinal properties, setting the stage for localized strategies to harness its full potential. This holistic approach systematically explores the chemistry and biological roles of *C. caesia*, thereby laying a foundation for its further

development in pharmaceutical and functional applications. With its unique phytochemical profile and 'magical' roots, *C. caesia* represents a promising natural resource for innovative healthcare solutions. Recent investigations have expanded the scope of its medicinal applications to include antiviral and antimicrobial activities. Essential oils and phytoconstituents extracted from its rhizomes have demonstrated efficacy against bacterial strains and viral pathogens, broadening its potential utility in treating infectious diseases (Chaturvedi et al., 2019; Pebam et al., 2022).

The integration of soil science and phytochemistry in this study offers a promising approach to optimizing the cultivation and therapeutic potential of *C. caesia*. By tailoring soil management practices, it is possible to enhance the yield of specific bioactive compounds, paving the way for their use in nutraceuticals, pharmaceuticals, and functional foods.

Materials and Methods

Chemicals and Reagents

The details of the solvents, reagents, and materials used are as follows:

- A. **Solvents:** Methanol, ethanol, petroleum ether, and hexane were procured from Thermo Fisher Scientific India, Powai, Mumbai.
- B. **Reagents:** Mayer's reagent, chloroform, acetic anhydride, ferric chloride, phenol solution, glucose, Folin-Ciocalteu's phenol reagent, sodium hydroxide, copper sulfate, gallic acid, potassium dichromate, formic acid, and acetonitrile were purchased from Merck Life Science Private Limited, Vikhroli, Mumbai.

- C. **Laboratory-Grade Chemicals:** Water (HPLC grade), sodium carbonate, and sodium potassium tartrate were obtained from Sisco Research Laboratories Pvt. Ltd., Turbhe, Mumbai.
- D. **Acids:** Hydrochloric acid and sulfuric acid were procured from Rankem, Thane, Mumbai.
- E. **Other Reagents:** Benedict's reagent was purchased from HIMEDIA Laboratories, Thane, Mumbai.

Sample Collection

Fresh rhizomes of *Curcuma caesia* Roxb. were collected from four distinct regions in Northeast India—Nongpoh (Meghalaya) Sample 1(refer S1(b)), Khetri (Assam) Sample 2 (refer S1(a)), Karbianglong (Assam) Sample 3 (refer S1(d)) and Moirang (Manipur) Sample 4 (refer S1(c)) —on August 17, 2022 (Figure 1).

For the pre-analysis preparation phase, the rhizomes were washed, oven-dried at 50°C, and powdered using a mechanical grinder. The powdered material was stored in airtight containers at 4°C to maintain stability before further analyses. The powdered rhizome samples (20 g each) were subjected to Soxhlet extraction using solvents of varying polarities, including petroleum ether, hexane, ethanol, and methanol. Each extraction cycle lasted 8 hours, and the solvent volume was maintained at 250 mL per cycle. The extracts were concentrated under reduced pressure using a rotary evaporator and stored at 4°C for further chemical analysis (refer S1(e)).

Soil Testing

Soil samples from the collection sites were analyzed to determine pH, nutrient content, and organic matter concentration. This analysis of soil testing data was performed to uncover the relationship between the environmental factors and the phytochemical profiles of the rhizomes.

Pharmacognostic Evaluation

Physical and Organoleptic Evaluation

The powdered rhizomes were subjected to visual and sensory analyses to assess color, texture, and odor. A microscopic examination was conducted to identify the presence of calcium oxalate crystals, parenchyma cells, and starch grains.

Microscopic Analysis

Powder microscopy revealed anatomical features such as xylem vessels, stone cells, and oleoresin crystals, which were indicative of the plant's identity and phytochemical composition.

Phytochemical Screening

Qualitative Analysis

Standard protocols were followed to identify the presence of alkaloids, flavonoids, tannins, reducing sugars, and steroids using chemical assays such as Mayer's test for alkaloids, the Shinoda test for flavonoids, Ferric chloride test for tannins and the Benedict's test for reducing sugars (Sahu et al., 2016).

Quantitative Analysis

The concentrations of carbohydrates, proteins, and phenols were estimated using the phenol-sulfuric acid, Lowry, and Folin-Ciocalteu methods, respectively. Lowery's procedure was used to determine the concentration of soluble protein. The absorbance was read at 560nm, and a standard graph comparing methanolic and ethanolic extracts was created by graphing the standard concentration on the X-axis against absorbance on the Y-axis. The total protein content was reported as equivalents regarding a standard curve ($Slope = 0.00008, Intercept = 0.0131, R^2 = 0.9777$)(Figure 2(a)).

The concentration of carbohydrates was estimated by following the standard phenol sulfuric acid protocol. Measurements of absorbance were taken at 490nm. A standard graph comparing methanolic and ethanolic extracts was generated by plotting the concentration of standards on the X-axis and absorbance on the Y-axis. The total carbohydrate content was expressed as glucose standard equivalent to a standard curve ($y = 0.0009x + 0.1448, R^2 = 0.9891$) (**Error! Reference source not found.**(b). The percentage of total carbohydrates present in 100ml of the sample solutions is calculated as $\left(\frac{x}{0.1}\right) \times 100$ mg of glucose.

At last, the concentration of phenol was estimated by following the Folin-Ciocalteu assay. The absorbance was read at 650nm by graphing the standard concentration on the X-axis against absorbance on the Y-axis, and a standard graph was created comparing both methanolic and ethanolic extracts. Gallic acid was given as the reported total phenolic content equivalence regarding a standard curve (standard curve equation: $y = 0.0011x + 1.3819, R^2 = 0.9878$)(Figure(2(c))).

Thin Layer Chromatography (TLC)

TLC was performed using ethanolic extracts to separate bioactive compounds. Solvent systems such as toluene, ethyl acetate, and methanol were used, and six distinct spots were observed under UV shortwave light with Rf Values: 0.11, 0.22, 0.28, 0.56, 0.64, and 0.88.

Curcumin Estimation

By refluxing the compound in alcohol, curcumin is quantitatively extracted and measured spectrophotometrically at 425 nm. 0.2–0.5 gms of weighed, dried black turmeric powdered was dissolved in 250 ml of pure ethanol. After refluxing the flask's contents over a heating element with the air condenser for three to five hours, replenish the flask with fresh alcohol to compensate for any evaporation loss. Once the extract cools down, transfer it into a volumetric flask and adjust the volume using 100% alcohol to dilute an appropriate portion (1-2 ml) to 10 ml. Using a spectrophotometer, determine the depth of the yellow hue at 425 nm. Curcumin content for both ethanol and methanol was estimated:

Calculation of curcumin concentration in the rhizome samples

$$CC = \frac{0.0025 \times A \times V \times DF}{W}$$

Where;

- CC is the curcumin concentration (g/100g)

- A is the absorbance 425nm.
- V is the volume
- DF is the dilution factor
- W is the sample's weight in gm

Physicochemical Analysis

Physicochemical parameters such as loss on drying (LOD), total ash, acid-insoluble ash, alcohol-soluble extractives, and water-soluble extractives were measured to assess the quality and purity of the plant material.

Structural and Chemical Characterization

FTIR Analysis

The Fourier transform infrared spectrophotometer (FTIR) is an effective tool for classifying the many types of functional groups found in plant extract by identifying chemical bonds. The dried powdered ethanolic and methanolic extract samples from 4 different regions were loaded in an FTIR Spectroscope. The scan detects numerous functional groups, including phenol, alkenes, and sulfoxide groups, through the Thermo Scientific FT-IR Spectrometer (Thermo Nicolet iS10) (Muthukumaran et al., 2017).

GC-MS Analysis

A 50 ml conical flask was filled with 40 ml of the solvent used during extraction, either ethanol or methanol. To this flask, 5g of the corresponding powder

extracts were added. The solution underwent sonication for 5 minutes, followed by concentration through the introduction of nitrogen gas bubbles. Later it was diluted with the suitable solvent as per extraction. 2 μ l of sample solution was injected into the gas chromatograph and recorded, and the retention time was compared with the NIST Database Library. The GC-MS analysis conditions are tabulated in **Error! Reference source not found.**

LC-MS

Liquid Chromatography-Mass Spectrometry (LC-MS) was used to identify non-volatile and thermolabile bioactive compounds. The analysis was performed using an Agilent 6224 TOF LC/MS system with a C4 column and a gradient method (mobile phases: H₂O + 0.1% formic acid, acetonitrile + 0.1% formic acid). The results were interpreted using Agilent MassHunter software.

Data Analysis

Statistical Analysis

All results were expressed as mean \pm standard deviation (SD) based on three replicates. Statistical significance was assessed using ANOVA ($p < 0.05$) and Student's t-tests ($p < 0.01$).

PCoA Analysis

Principal Coordinates Analysis (PCoA) was performed to visualize the variability in the phytochemical composition of samples from the four locations. The analysis was based on a matrix of functional groups and bioactive compounds such as protein, carbohydrate, phenolic content, and curcumin concentration identified through FTIR, GC-MS, and LC-MS (refer Figure 3).

Correlation Analysis

To investigate the relationship between curcumin concentration in *Curcuma caesia* rhizomes and various soil parameters (e.g., pH, organic carbon, nutrient levels), a correlation analysis was performed. Soil data, including pH, organic carbon, nitrogen, phosphorus, potassium, calcium, magnesium, sulfur, chloride, and moisture, were evaluated for their influence on curcumin concentration. Pearson's correlation coefficients were calculated to determine the strength and direction of the relationships.

The analysis was performed using Python (v3.x) with libraries including pandas for data handling, numpy for mathematical operations, and seaborn/matplotlib for data visualization. The interpretation of the correlation coefficients is done based on 3 conditions, where values close to **1** indicate a strong positive relationship, i.e., both variables (e.g., curcumin concentration increases with increase in soil's N, P or K contents). Meanwhile values close to **-1** indicate a strong negative relationship (e.g., one variable decreases as the other increases). At last are the values near **0**, which suggest little to no linear relationship.

Results

The soil sampling analysis showed clear differences across the four regions. The least acidic soil was observed in Nongpoh, with a neutral to slightly alkaline pH of 7.13, while its organic carbon content was moderate at 2.11%. Nitrogen levels in Nongpoh were relatively high at 314.12 ppm, and phosphorus levels were the second highest of all samples at 95 ppm. Potassium content was 131.25 ppm, and calcium was the highest of all locations, recorded at 521.04 ppm. Magnesium was also highest in Nongpoh at 389.12 ppm, while sulfur was the highest at 185 ppm. Chloride levels were highest at 198.8 ppm. Moisture content in Nongpoh was moderate at 8.6% (Table 2).

Khetri had a slightly acidic pH of 6.28 and the highest organic carbon of all samples at 3.55%. Nitrogen was the highest among all regions at 527.48 ppm, while phosphorus was also the highest at 99 ppm. Potassium showed the most significant value of 1206.25 ppm, the highest of all samples. Calcium was 440.88 ppm, while magnesium was recorded at 364.8 ppm. Sulfur levels were 89.49 ppm, and chloride was the lowest among the four regions at 49.7 ppm. Moisture content was the lowest of all regions at 1.45%.

Karbianglong had a moderately acidic pH of 5.91, with organic carbon at 1.88%. Nitrogen levels were 278.56 ppm, and phosphorus content was 42.5 ppm. Potassium was the lowest of all regions at 95 ppm, and calcium was recorded at 480.96 ppm. Magnesium was moderate at 267.52 ppm, while sulfur content was 16.41 ppm. Chloride was 149.1 ppm, and moisture content was recorded at 5.83%.

Lastly, Moirang had the most acidic soil of all locations, with a pH of 4.09. Organic carbon was the lowest among all samples at 1.56%, and nitrogen levels were also the lowest at 231.14 ppm. Phosphorus was the lowest of all regions at 22 ppm, while potassium was moderate at 171.25 ppm. Calcium was the lowest among all samples at 80.16 ppm, and magnesium was also the lowest at 194.56 ppm. Sulfur was entirely absent, while chloride levels were 63.9 ppm. Moirang had the highest moisture content of all locations, recorded at 27.86% (Figure 4).

The qualitative screening for phytochemical compounds (Table 3) showed consistent results across all samples from Nongpoh, Khetri, Karbianglong, and Moirang (Table 4). Alkaloids, flavonoids, reducing sugars, steroids, and tannins were present in all samples, with no observed variation among the regions.

The quantitative estimation of phytochemical components revealed that the ethanolic extract from Moirang exhibited the highest overall protein concentration among all regions (17.85 ± 0.01 mg/ml), followed by Khetri (16.54 ± 0.01 mg/ml), Karbianglong (12.32 ± 0.01 mg/ml), and Nongpoh (9.6 ± 0.44 mg/ml).

Carbohydrate content was highest in Moirang's ethanolic extract (4.29 ± 0.02 mg/ml), followed by Nongpoh (4.25 ± 0.02 mg/ml), Karbianglong (4.05 ± 0.02 mg/ml), and Khetri (3.94 ± 0.03 mg/ml). Phenolic content in ethanolic extracts was lowest in Nongpoh (0.15 ± 0.01 mg/ml) and highest in Moirang (0.71 ± 0.01 mg/ml). Khetri and Karbianglong showed similar phenolic levels, at 0.69 ± 0.01 mg/ml and 0.7 ± 0.01 mg/ml, respectively. Curcumin content was highest in Moirang's ethanolic extract (0.0117 ± 0.00 g), followed by Khetri (0.0093 ± 0.00 g), Karbianglong (0.0079 ± 0.00 g), and Nongpoh (0.0023 ± 0.00 g) (Table 5).

The FTIR analysis identified eight functional groups across the samples. In Nongpoh, secondary alcohols and aliphatic amines were detected, while sulfoxides and phenols were absent. Khetri exhibited a wide range of functional groups, including phenols and sulfoxides, which were also present in Karbianglong. Moirang showed functional groups like sulfoxides and secondary alcohols, but phenols were absent (Table 6–7, Figure 5).

The GC-MS analysis identified 18 bioactive compounds across the ethanolic extracts. In Nongpoh, curcumenol (16.01%) and curcumenone (16.88%) were prominent, with benzofuran (5.73%) also detected. Khetri showed similar trends, with epicurzerenone (41.2%) and furanodienone (35.18%) as dominant compounds. Karbianglong also exhibited curcumenol and curcumenone as significant compounds. Moirang had higher proportions of benzofuran and other bioactive compounds compared to the other regions (Table 8, Figures 5–7).

The LC-MS analysis revealed nine non-volatile compounds. Nongpoh showed the presence of curcumin, hinokinin, and pyropheophorbide a. Khetri identified similar compounds, with curcumin as the most prominent. Karbianglong also exhibited consistent results, with hinokinin and luteone identified (Table 9). Moirang showed the highest concentrations of curcumin and melilotoside A2 among the regions.

Correlation analysis showed that curcumin concentration (g) has a strong negative correlation with pH (-0.8645), sulfur (-0.8735), and chloride (-0.8903), suggesting that higher levels of these parameters may reduce curcumin synthesis. In contrast, curcumin is strongly positively correlated with protein (0.9414) and phenolic content (0.9262). Phenolic content shows strong positive correlation with curcumin (0.9262)

and protein (0.7883) but negative correlations with sulfur and chloride. Principal Coordinate Analysis (PCoA) (Figure 3) highlighted variability among the four regions, with PC1 accounting for 61.28% of variance and PC2 for 22.26%, showing distinct clustering patterns among samples.

Discussion

The results demonstrate that soil characteristics strongly influence the phytochemical profile of *Curcuma caesia* across regions. The acidic soils of Moirang corresponded with the highest curcumin and phenolic content, while Nongpoh's near-neutral pH correlated with the lowest levels. This aligns with earlier findings that acidic soils favor phenolic and flavonoid synthesis due to enhanced nutrient solubility and root uptake efficiency (Sandeep et al., 2015; Pebam et al., 2022).

The strong negative correlation between curcumin and pH confirms that acidic conditions enhance curcumin biosynthesis, possibly by stimulating enzymatic pathways associated with phenolic metabolism (Klimiené et al., 2021). Likewise, the positive relationship between curcumin, protein, and phenolic content indicates shared biosynthetic pathways modulated by soil nutrients and organic matter.

The FTIR, GC-MS, and LC-MS analyses collectively confirm the presence of bioactive compounds such as curcumenol, curcumenone, benzofuran, and curcumin, which contribute to the plant's medicinal potential. The high diversity of compounds in the ethanolic extracts suggests that solvent polarity significantly influences extraction efficiency and compound yield (Muthukumaran et al., 2017; Chaturvedi et al., 2019).

Furthermore, the clustering observed in PCoA emphasizes regional chemotypic differentiation, implying that *C. caesia* adapts metabolically to its soil environment. Such ecological specialization supports localized cultivation strategies to enhance desired bioactive profiles. These findings also validate traditional claims regarding the superior therapeutic quality of *C. caesia* from specific regions of Northeast India (Haida et al., 2023; Paudel et al., 2024).

Overall, this study establishes a holistic link between soil parameters and medicinal compound biosynthesis, offering a framework for targeted cultivation of *C. caesia* for pharmaceutical and nutraceutical use. Future research should focus on molecular-level analysis of gene–environment interactions and in vivo validation of therapeutic activities to substantiate the pharmacological relevance of these phytochemicals.

Author Contribution Statement:

Rana Mukherjee – Conceptualization, Methodology, Data Analysis, Writing – Original Draft.

Deboja Sharma (Corresponding Author) – Conceptualization, Supervision, Writing – Review & Editing.

Ankita Kalita – Data Collection, Analysis, Writing – Original Draft.

Subhadeep Sarkar – Data Collection, Review & Editing.

Gauri Dutt Sharma – Visualization, Writing – Review & Editing.

All authors have read and approved the final manuscript.

Funding Source of Research:

This research did not receive any specific funding from public, commercial, or not-for-profit agencies.

Acknowledgements:

The authors thank the Applied Biology Department, Advanced Research Centre (USTM), and Guwahati Biotech Park for their support. Special thanks to Mr. Bhagwan Boro for his assistance during sample collection. Additionally, we acknowledge ProwessisAI Solutions for their assistance in data analysis and statistical evaluation.

Conflict of Interest:

The authors declare no known competing financial interests or personal relationships that could have appeared to influence the work reported in this paper.

References:

1. Chaturvedi, M., Rani, R., Sharma, D., & Yadav, J. P. (2019). Comparison of *Curcuma Caesia* extracts for bioactive metabolite composition, antioxidant and antimicrobial potential. *Natural Product Research*, 35(18), 3131–3135. <https://doi.org/10.1080/14786419.2019.1687472>
2. Devi, H. P., & Mazumder, P. B. (2016). Methanolic Extract of *Curcuma caesia* Roxb. prevents the toxicity caused by Cyclophosphamide to bone marrow cells, liver and kidney of mice. *Pharmacognosy Research*, 8(1), 43–43. <https://doi.org/10.4103/0974-8490.171106>

3. Devi, H. P., Mazumder, P. B., & Devi, L. P. (2015). Antioxidant and antimutagenic activity of *Curcuma caesia* Roxb. rhizome extracts. *Toxicology Reports*, 2, 423–428. <https://doi.org/10.1016/j.toxrep.2014.12.018>
4. Dosoky, N. S., & Setzer, W. N. (2018). Chemical Composition and Biological Activities of Essential Oils of *Curcuma* Species. *Nutrients*, 10(9), 1196–1196. <https://doi.org/10.3390/nu10091196>
5. Elhawary, S. S., Radwan, R. A., & Khalil, M. M. (2024). A comprehensive review of bioactive compounds in the genus *Curcuma*: Phytochemistry and pharmacological insights. *Journal of Ethnopharmacology*, 125(2), 125–138. <https://doi.org/10.1016/j.jep.2024.01.006>
6. Haida, Z., Nakasha, J. J., Sinniah, U. R., & Hakiman, M. (2023). Ethnomedicinal uses, phytochemistry, pharmacological properties, and toxicology of *Curcuma caesia* Roxb.: A review. *Advances in Traditional Medicine*, 23(985–1001). <https://doi.org/10.1007/s13596-022-00685-7>
7. Haruna, A., & Yahaya, S. M. (2021). Recent Advances in the Chemistry of Bioactive Compounds from Plants and Soil Microbes: a Review. *Chemistry Africa*, 4(2), 231–248. <https://doi.org/10.1007/s42250-020-00213-9>
8. Klimienė, A., Klimas, R., Shutava, H., & Razmuvienė, L. (2021). Dependence of the Concentration of Bioactive Compounds in *Origanum vulgare* on Chemical Properties of the Soil. *Plants*, 10(4), 750–750. <https://doi.org/10.3390/plants10040750>

9. Muthukumaran P, Kalakandan S.K and Ravichandran K (2017). Phytochemical Screening, GC-MS, FT-IR Analysis of Methanolic Extract of *Curcuma caesia* Roxb (Black Turmeric). *Pharmacog J*.9(6):952-6. doi:[10.5530/pj.2017.6.149](https://doi.org/10.5530/pj.2017.6.149)
10. Paudel, A., Khanal, N., Khanal, A., Rai, S., & Adhikari, R. (2024). Pharmacological insights into *Curcuma caesia* Roxb., the black turmeric: a review of bioactive compounds and medicinal applications. *Discover Plants*, 1, 69. <https://doi.org/10.1007/s44372-024-00076-1>
11. Pebam, M., Yumnam, S., Singh, T. S., & Devi, N. P. (2022). Environmental and soil factors affecting phytochemical content and bioactivity of *Curcuma caesia* from Northeast India. *International Journal of Medicinal Plants*, 3(4), 122–133. <https://doi.org/10.1186/s43538-022-00099-w>
12. Rahaman, M. M., Rakib, A., Mitra, S., Tareq, A. M., Emran, T. B., Shahid-Ud-Daula, A. F. M., Amin, M. N., & Simal-Gandara, J. (2020). The Genus *Curcuma* and Inflammation: Overview of the Pharmacological Perspectives. *Plants*, 10(1), 63–63. <https://doi.org/10.3390/plants10010063>
13. Raj, A. J., Biswakarma, S., Pala, N. A., Shukla, G., Vineeta, Kumar, M., Chakravarty, S., & Bussmann, R. W. (2018). Indigenous uses of ethnomedicinal plants among forest-dependent communities of Northern Bengal, India. *Journal of Ethnobiology and Ethnomedicine*, 14(1), 8. <https://doi.org/10.1186/s13002-018-0208-9>
14. Sandeep, I., Nayak, & Mohanty, S. (2015). Differential effect of soil and environment on the metabolic expression of turmeric (*Curcuma longa* cv. Roma). *Indian Journal of Experimental Biology*, 53, 406–411.

[https://nopr.niscpr.res.in/bitstream/123456789/31582/1/IJEB%2053\(6\)%20406-411.pdf](https://nopr.niscpr.res.in/bitstream/123456789/31582/1/IJEB%2053(6)%20406-411.pdf)

Tables

Table 1

GC-MS: Chromatographic conditions

Column	DB-FFAP (30M x 0.530mm x 1.0 μ m)
Column initial temperature	100°C
Column initial time	6 min
Program rate	15 ⁰ /min
Column final temperature	200°C
Column final time	9 min
Injector temperature	220°C
Detector temperature	270°C
Equilibrium time	0.2 min
Attenuation	-3
Range	1
Run time	40 min
Split flow	20 ml/min
Injection volume	2 μ l
Mode	Flow
Hydrogen gas	30.0 ml/min
Nitrogen carrier gas	2 ml/min
Helium gas	300 ml/min

Table 2

Soil sample analysis report

Parameter	Karbianglong	Moirang	Nongpoh	Khetri
pH	5.91	4.09	7.13	6.28
Organic Carbon (%)	1.88	1.56	2.11	3.55
Nitrogen (ppm)	278.56	231.14	314.12	527.48
Phosphorus (ppm)	42.5	22	95	99
Potassium (ppm)	95	171.25	131.25	1206.25
Calcium (ppm)	480.96	80.16	521.04	440.88
Magnesium (ppm)	267.52	194.56	389.12	364.8
Sulfur (ppm)	16.41	0	185	89.49
Chloride (ppm)	149.1	63.9	198.8	49.7
Iron (ppm)	6	8.4	10.8	10.8
Manganese (ppm)	34.4	51.6	34.4	51.6
Sodium (ppm)	182.5	67.5	181.25	113.75
Moisture (%)	5.83	27.86	8.60	1.45

Table 3*Phytochemical compounds studied in this article*

Compound Name	PubChem CID
1,2-Dihydrovomilenine	11953964
2,3-Dehydrokievitone	5746354
13-HPODE	6437847
Ambrosin	92119
Azulen	9231
Benzofuran	9223
Bornyl acetate	93009
Camphor	2537
Caryophyllene oxide	1742210
Curcumenol	167812
Curcumenone	14632994
Curcumin	969516
Cyclohexane	8078
Epicurzerenone	5317062
Eucalyptol	2758
Furanodienone	6442374
Hinokinin	442879
Lidocaine	3676
Linalool	6549
Luteone	5281797
Melilotoside A2	13632905

Pyropheophorbidea	161456
Sesamin	72307
Stigmasterol	5280794
Zederone	71694446
β-Sitosterol	481107734

Table 4

Qualitative Phytochemical Screening Results

Test	Karbianglong	Moirang	Nongpoh	Khetri
Alkaloids	+Ve	+Ve	+Ve	+Ve
Flavonoids	+Ve	+Ve	+Ve	+Ve
Reducing Sugars	+Ve	+Ve	+Ve	+Ve
Steroids	+Ve	+Ve	+Ve	+Ve
Tannins	+Ve	+Ve	+Ve	+Ve

Table 5

Combined Estimation of Phytochemical Components Across Different Locations and Extraction Methods

Compound Estimated	Ethanol	Methanol	Petroleum Ether	Hexane
Protein				
Karbianglong	12.32 ± 0.01	10.19 ± 0.01	7.52 ± 0.03	1.75 ± 0.01
Moirang	17.85 ± 0.01	17.06 ± 0.01	5.31 ± 0.02	5.56 ± 0.01
Nongpoh	9.6 ± 0.44	16.77 ± 0.01	4.28 ± 0.02	1.81 ± 0.01
Khetri	16.54 ± 0.01	16.69 ± 0.01	7.97 ± 0.02	5.6 ± 0.43
Carbohydrate				
Karbianglong	4.05 ± 0.02	4.28 ± 0.02	4.16 ± 0.03	4.23 ± 0.03
Moirang	4.29 ± 0.02	4.22 ± 0.03	4.18 ± 0.03	4.28 ± 0.02
Nongpoh	4.25 ± 0.02	3.28 ± 0.03	4.03 ± 0.03	4.28 ± 0.04
Khetri	3.94 ± 0.03	3.95 ± 0.02	4.27 ± 0.02	4.27 ± 0.02
Phenolic				
Karbianglong	0.7 ± 0.01	0.33 ± 0.01	1.19 ± 0.01	1.01 ± 0.005
Moirang	0.71 ± 0.01	0.31 ± 0.01	1 ± 0.00	0.94 ± 0.005
Nongpoh	0.15 ± 0.01	0.28 ± 0.01	1.07 ± 0.01	1.12 ± 0.005
Khetri	0.69 ± 0.01	0.16 ± 0.01	1.04 ± 0.01	0.94 ± 0.005
Curcumin				
Karbianglong	0.0079 ± 0.00	0.00025 ± 0.00	-	-
Moirang	0.0117 ± 0.00	0.0003 ± 0.00	-	-

Nongpoh	0.0023	±	0.00014	±	-	-
	0.00		0.00			
Khetri	0.0093	±	0.00032	±	-	-
	0.00		0.00			

Table 6

Results of the FTIR

S. No.	Retention Time (RT)	Name of Compound	Molecular Formula	Molecular Weight (g/mol)	Peak Area (%)
1	7.83	Eucalyptol	C10H18O	154.25	0.61
2	8.85	Linalool	C10H18O	154.25	0.95
3	9.575	Camphor	C10H16O	152.23	0.85
4	11.255	Bornyl acetate	C12H20O2	196.29	0.88
5	12.309	Cyclohexane, 1-ethenyl-1-methyl-2,4-bis(1-methylethenyl)-	C15H24	204.35	1.6
6	13.268	Benzofuran	C8H6O	118.13	5.73
7	14.163	Furanodienone	C15H18O2	230.3	35.18
8	14.194	Epicurzerenone	C15H18O2	230.3	41.2
9	15.217	Curcumenol	C15H22O2	234.33	16.01
10	15.221	Azulen-2-ol	C10H8O	144.17	0.89
11	15.911	Curcumenone	C15H22O2	234.33	16.88
12	16.027	Caryophyllene oxide	C15H24O	220.35	1.2
13	16.333	Lidocaine	C14H22N2O	234.34	0.98
14	17.051	Ambrosin	C15H18O3	246.3	8.55
15	17.55	Picrotoxinin	C15H16O6	292.28	1.15
16	18.891	Zederone	C15H18O3	246.3	2.71
17	28.764	Stigmasterol	C29H48O	412.7	0.86
18	30.141	β-Sitosterol	C29H50O	414.7	0.96

Table 7

FTIR Functional Group Identification using Ethanol extract

Range	Bond	Characteristic	MAE	NPE	KHE	KAE
3450-3200	O-H Stretching	Phenols		Positive		
3000-2850	C-H Stretching	Alkane	Positive		Positive	Positive
1390-1310	O-H Bending	Phenol	Positive		Positive	
1340-1250	CN stretch	Aromatic primary amine				

1250-1020	C-N Stretching	Aliphatic-amine		Positive	Positive
1124-1087	C-O Stretching	Secondary-alcohol	Positive	Positive	Positive
1070-1030	S=O Stretching	Sulfoxide	Positive	Positive	
1000-650	=C-H Bending	Alkenes	Positive	Positive	Positive
1150-500	C-X	Alkyl Halides		Positive	Positive

Table 8

GC-MS Analysis: Identified Compounds

Compound Name	Molecular Formula	Molecular Weight (g/mol)	Retention Time (RT)	Activity
Eucalyptol	C ₁₀ H ₁₈ O	154.25	7.83	Anti-inflammatory cytokine inhibitor
Linalool	C ₁₀ H ₁₈ O	154.25	8.85	Antimicrobial and antifungal
Curcumenol	C ₁₅ H ₂₂ O ₂	234.33	15.217	Anti-inflammatory, anti-tumor
Benzofuran	C ₈ H ₆ O	118.13	13.268	Anti-tumour, antibacterial
β-Sitosterol	C ₂₉ H ₅₀ O	414.7	30.141	Preventing skin aging

Table 9

LC-MS Analysis: Identified Compounds

Peak Number	Compound	Elemental Composition	Calculated Mass	Retention Time (min)	Activity
1	Hinokinin	C ₂₀ H ₁₈ O ₆	319.094075	0.40583	Antiprotozoal agents and antifungal agents
2	Luteone	C ₂₀ H ₁₈ O ₆	319.094075	0.40583	Preinfectional antifungal agent
3	2,3-Dehydrokievitone	C ₂₀ H ₁₈ O ₆	319.094075	0.40583	Antibacterial agent
4	Sesamin	C ₂₀ H ₁₈ O ₆	319.094075	0.40583	Antioxidant and anti-inflammatory

5	1,2-Dihydrovomilenine	C21H24N2O3	317.167753	0.4735	Antibacterial and antifungal agents
6	Pyropheophorbide a	C33H34N4O3	535.269638	0.0506	Anticancer and antiviral activities
7	Curcumin	C21H20O6	333.11242	0.13518	Antioxidant and reduces inflammation
8	Melilotoside A2	C36H58O9	673.374877	0.33817	Antioxidant, anti-inflammatory, antiproliferative effects
9	13-HPODE	C18H32O4	351.192298	0.45657	Pro-inflammatory activity in immune cells

Figure captions

S1(a): Black Turmeric from Khetri

S1(b): Black Turmeric from Nongpoh

S1(c): Black Turmeric from Moirang

S1(d): Black Turmeric from Karbianglong

S1(e). Flowchart diagram of sample collection, preparation, and extraction

Figure 1: Geolocations of the sample collection (sites) mapped to their respective six-digit coordinates

Figure 2(a): Standard curve of BSA

Figure 2(b): Standard curve of Glucose

Figure 2(c): Standard curve of Gallic acid

Figure 3: PCoA Analysis

Figure 4: Correlation plot of phytochemicals versus soil elements

Figure 5: FTIR analysis of *Curcuma caesia* Roxb of ethanolic extraction

Figure 6 :GC-MS analysis of *Curcuma caesia* Roxb of ethanolic extraction

Figure 7: 2D structure of identified molecules from *C. caesia* using GC-MS analysis

Figure 8 :Curcumin Estimation

Figure 9: Quantitative Phenolic Estimation

Figure 10 :Quantitative Protein Estimation

Arabic Summary (الملخص العربي)

الملخص العربي

وهو نبات طبي نادر من شمال (Curcuma caesia Roxb.) تم إجراء هذه الدراسة على نبات الكركم الأسود شرق الهند، بهدف تحليل مكوناته الكيميائية النباتية ودراسة تأثير خصائص التربة على تراكيز المركبات النشطة جُمعت عينات من أربعة مواقع مختلفة هي كاربينجلونج، مويرنج، نونجوبه، وخيتري، وتم تحليلها بيولوجياً فيه (FTIR)، باستخدام طرق متقدمة مثل الاستخلاص بجهاز سوكسلت، التحليل الطيفي بالأشعة تحت الحمراء والكروماتوغرافيا السائلة المقترنة بمطياف الكتلة (GC-MS)، الكروماتوغرافيا الغازية المقترنة بمطياف الكتلة (LC-MS).

وتسعة مركبات غير متطابقة GC-MS أظهرت النتائج وجود ثمانية عشر مركباً فعالاً تم تحديدها بواسطة كما أظهرت عينات مويرنج أعلى من بينها الكركومين، الكامفور، اللينالول، والبنزوفوران، LC-MS بواسطة وأعلى تركيز من الفينولات والبروتينات، في حين كانت عينات نونجوبه (جم 0.0117) محتوية من الكركومين الأقل من حيث المحتوى الحيوي.

أشارت نتائج تحليل التربة إلى أن التربة الحمضية الغنية بالمواد العضوية ترتبط بزيادة إنتاج المركبات الفينولية وجود تمايز واضح بين المناطق من حيث خصائص (PCoA) كما أوضحت التحاليل الإحصائية. والكركومين التربة والتركيب الكيميائي للنبات.

تؤكد هذه الدراسة الدور الحيوي للعوامل البيئية في تعزيز النشاط الدوائي لنبات الكركم الأسود، وتقدم إطاراً علمياً لتحسين ممارسات الزراعة المستدامة وتطوير الاستخدامات الصيدلانية والغذائية لهذا النبات ذي القيمة العالية.

خصائص التربة، التحليل الكيميائي النباتي، النشاط، Curcuma caesia، الكركم الأسود، الكلمات المفتاحية: الحيوي، شمال شرق الهند، النباتات الطبية.

Referees

Please consider the following potential referees for this manuscript:

Dr. Alok Bharadwaj, Ph.D.
Assistant Professor,
GLA University, India
Email: alok.bharadwaj@gla.ac.in

Dr. Samir Das, Ph.D.
Postdoctoral Fellow,
Chulalongkorn University, Thailand
Email: drsamirvph@yahoo.com

Figures



S1(a): Black Turmeric from Khetri



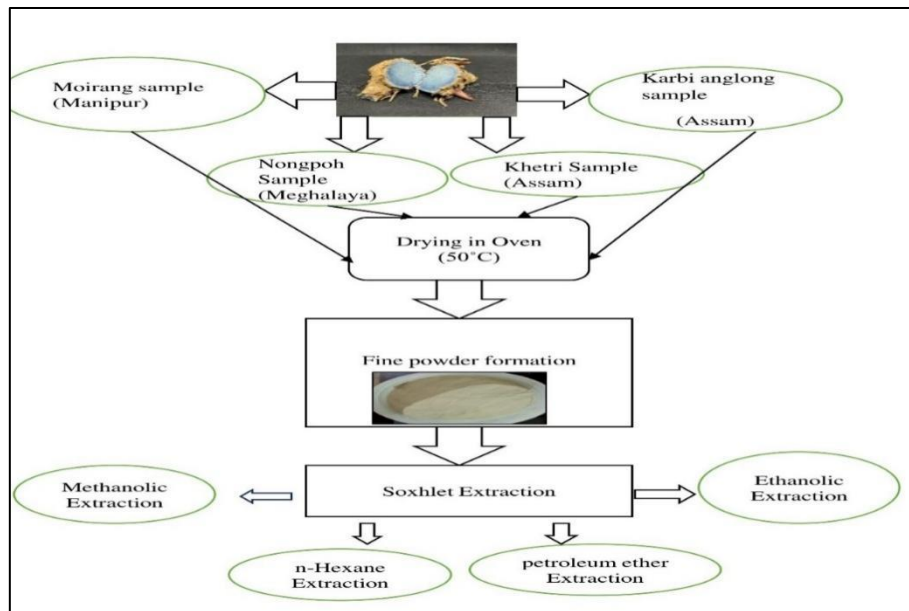
S1(b): Black Turmeric from Nongpoh



S1(c): Black Turmeric from Moirang



S1(d): Black Turmeric from Karbianglong



S1(e). Flowchart diagram of sample collection, preparation, and extraction



Figure 1: Geolocations of the sample collection (sites) mapped to their respective six-digit coordinates

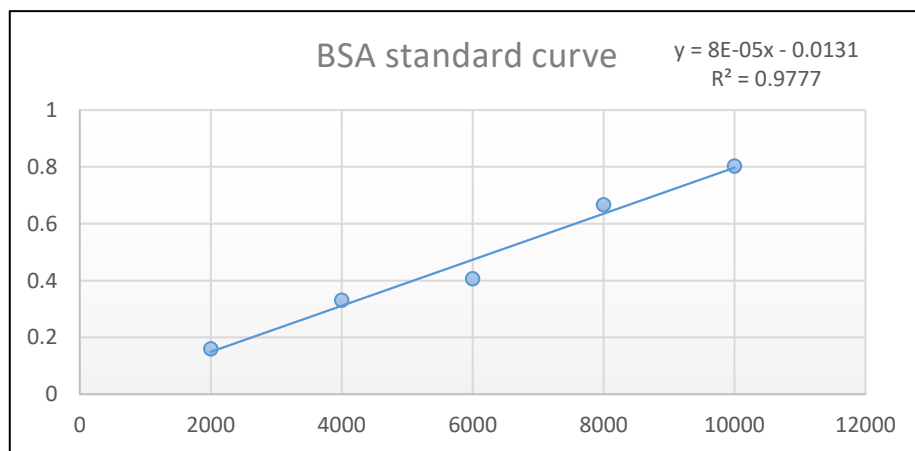


Figure 2(a): Standard curve of BSA

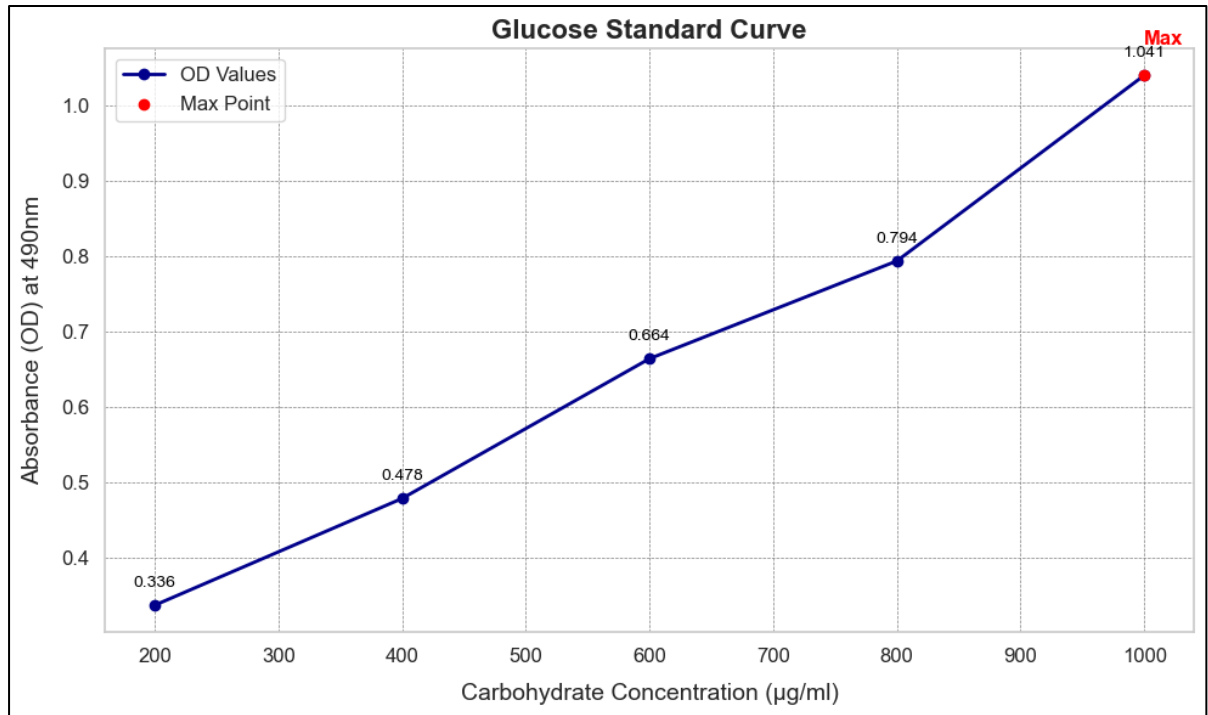


Figure 2(b): Standard curve of Glucose

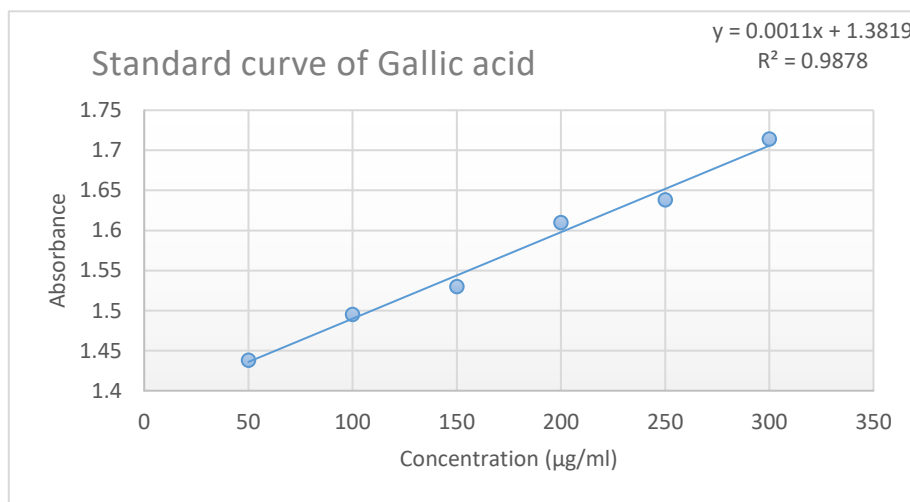


Figure 2(c): Standard curve of Gallic acid

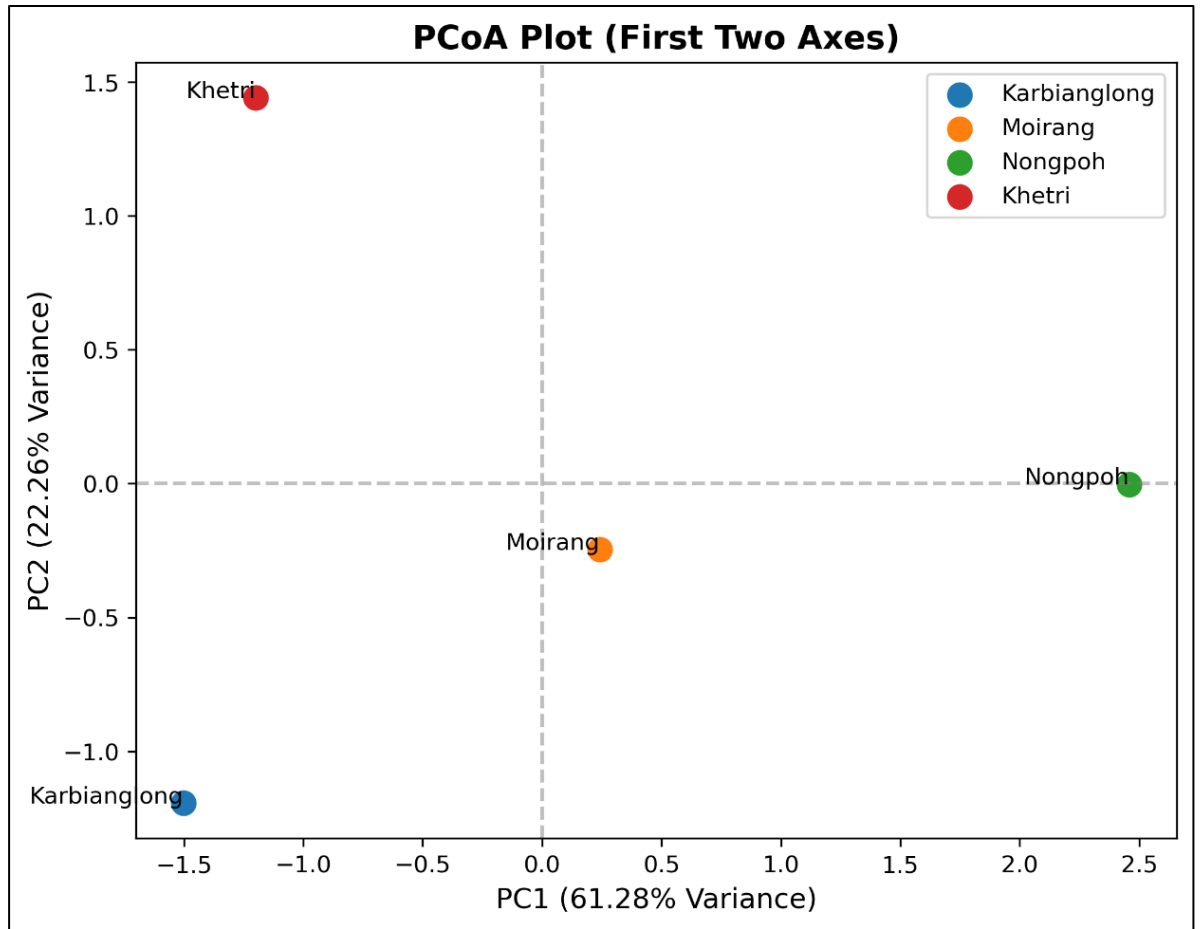


Figure 3: PCoA Analysis

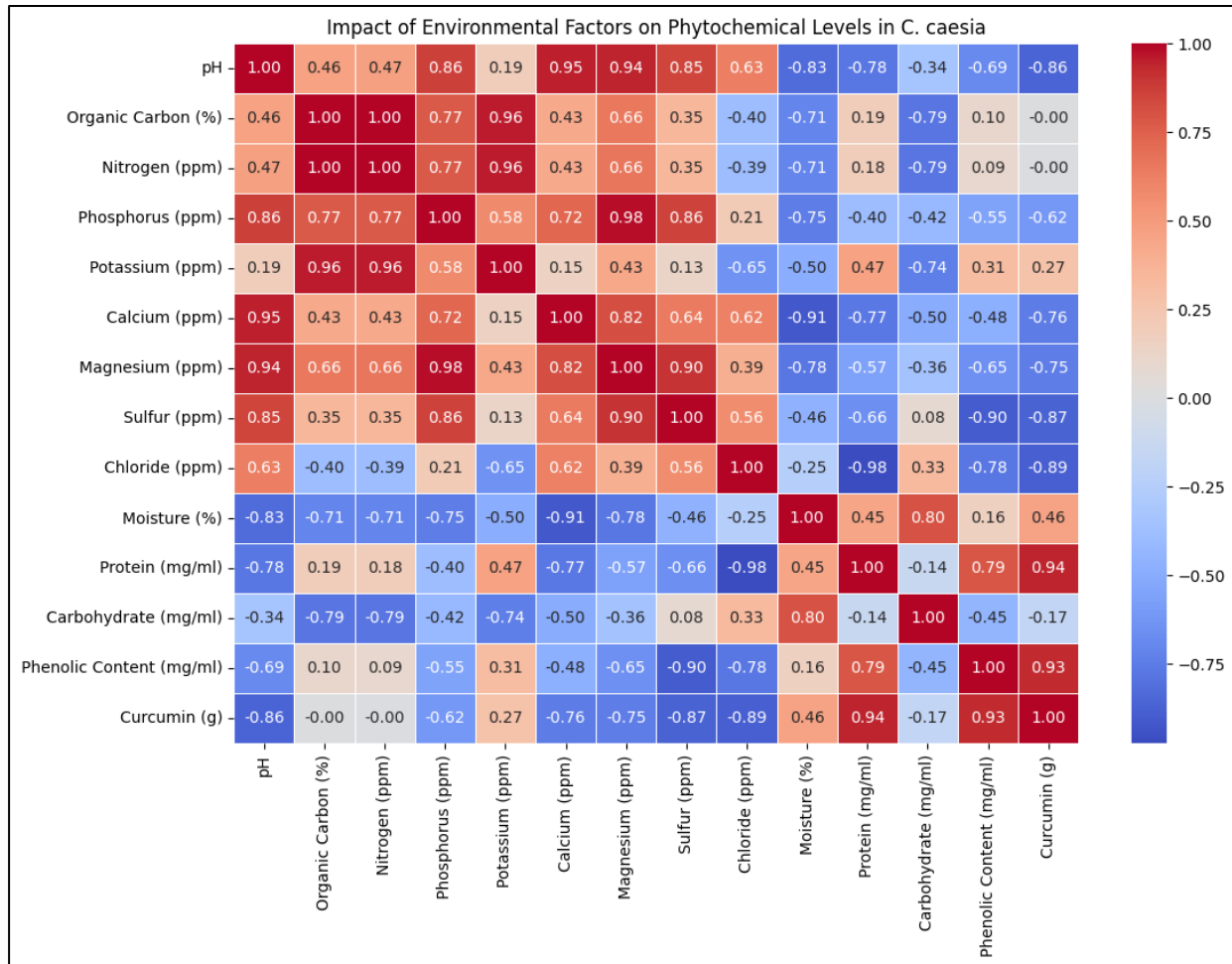


Figure 4: Correlation plot of phytochemicals versus soil elements

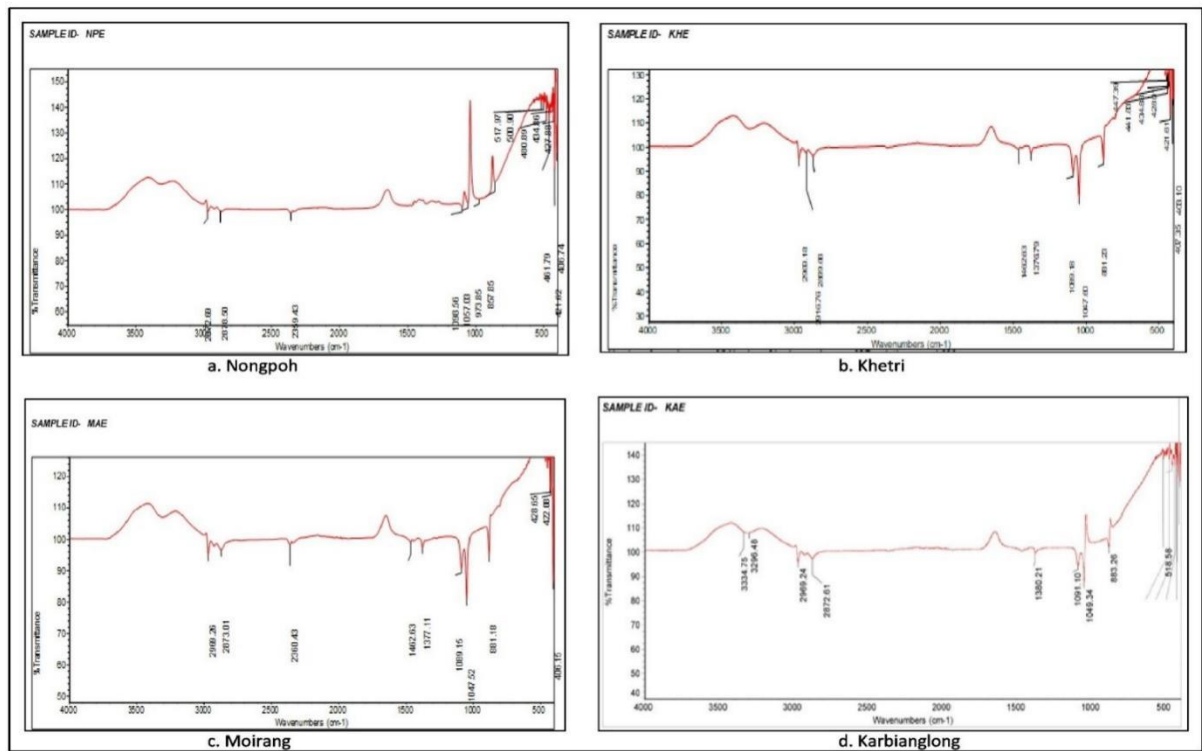


Figure 5:FTIR analysis of Curcuma caesia Roxb of ethanolic extraction

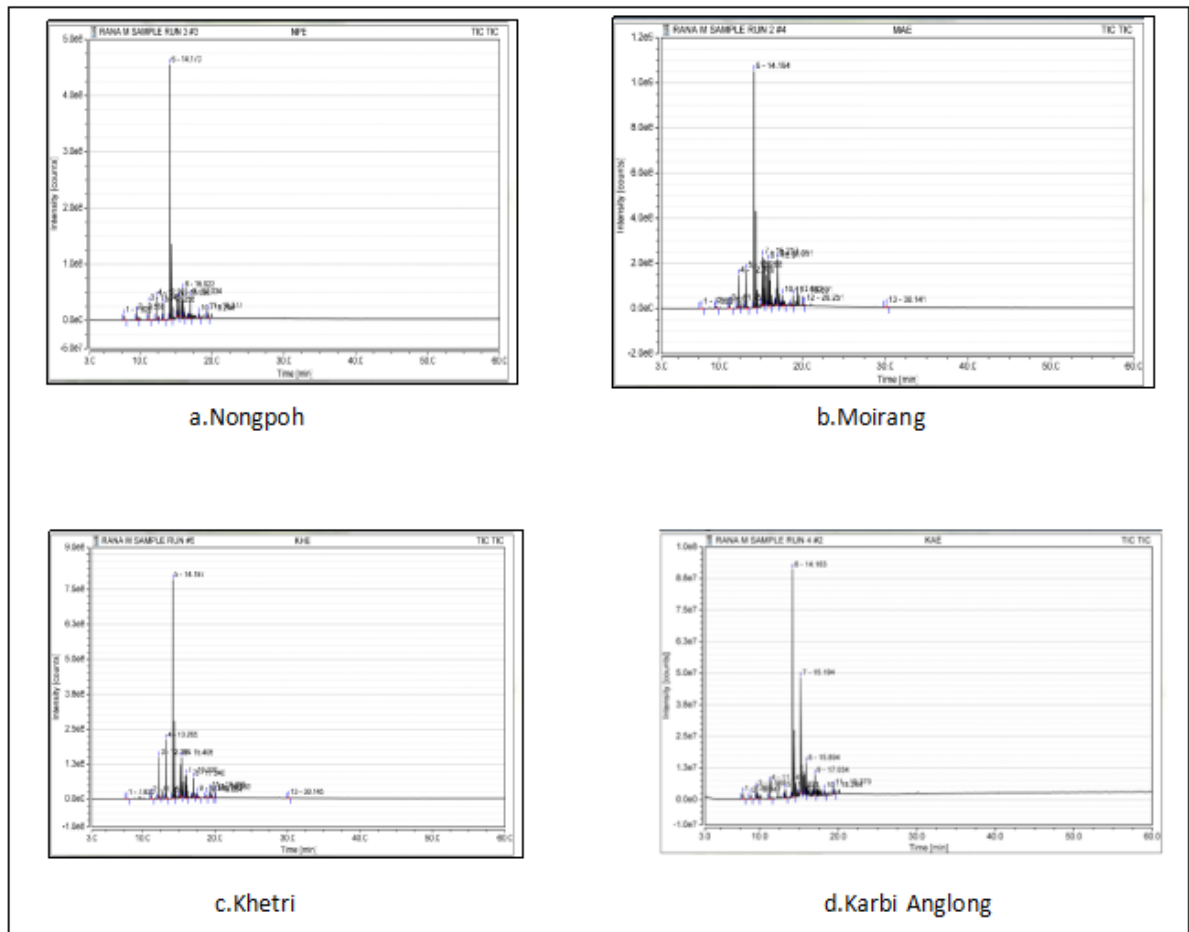


Figure 6 :GC-MS analysis of Curcuma caesia Roxb of ethanolic extraction

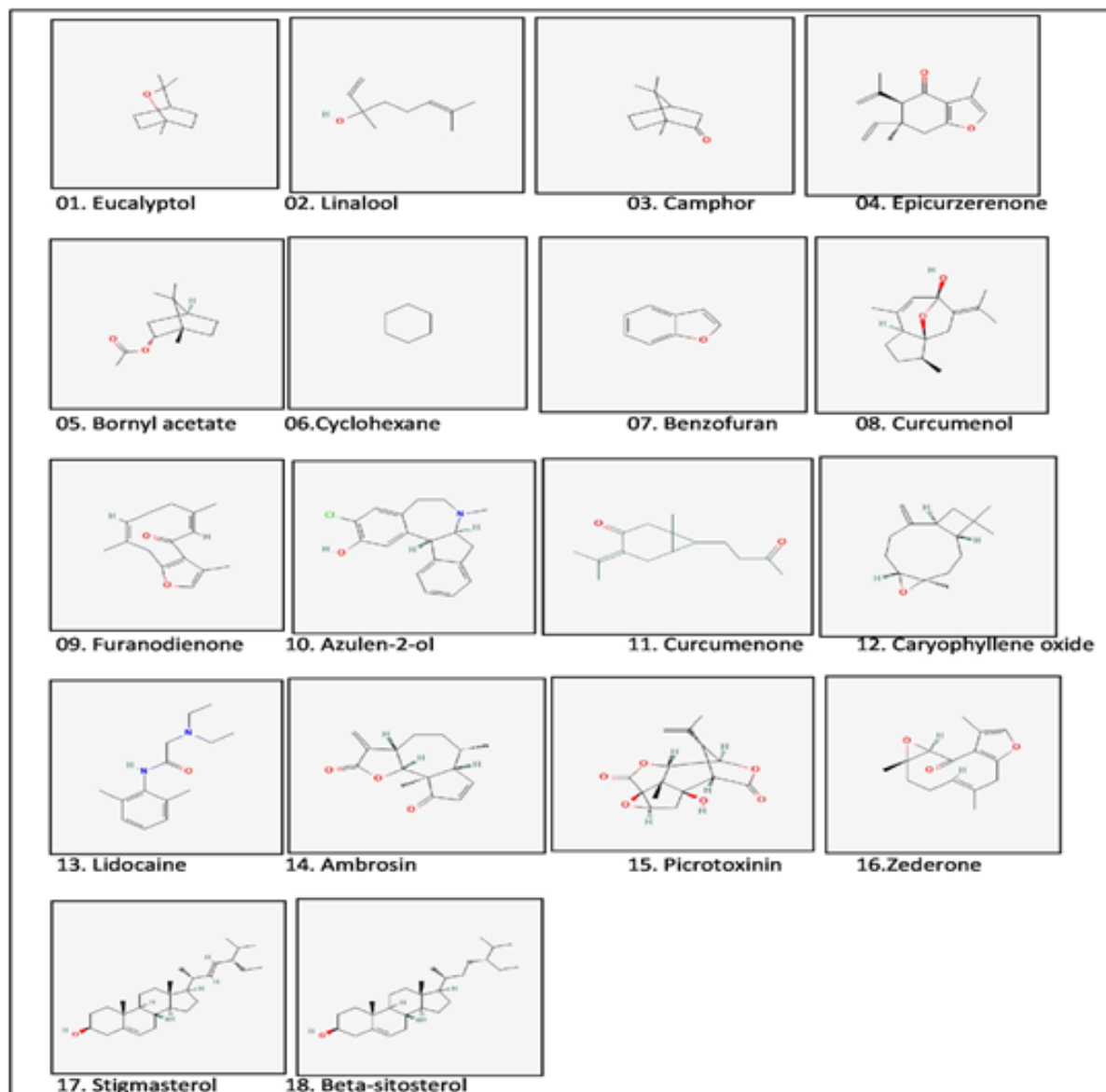


Figure 7:2D structure of identified molecules from *C. caesia* using GC-MS analysis

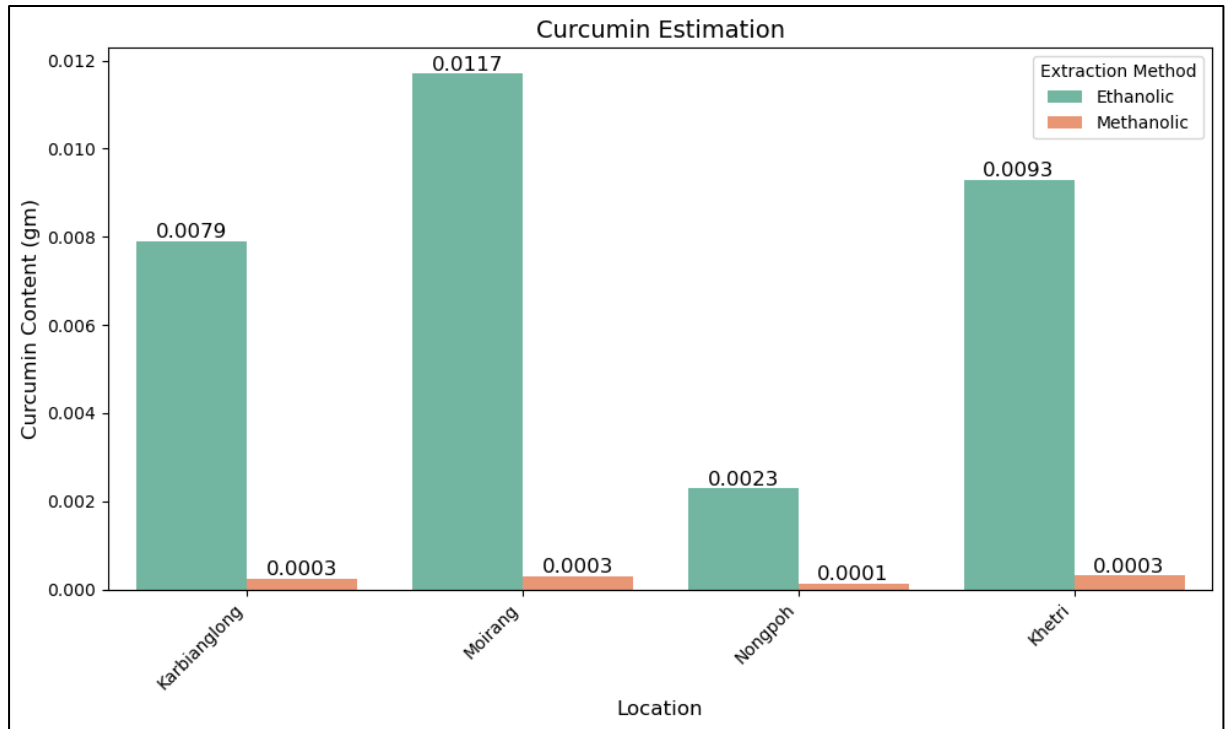


Figure 8 :Curcumin Estimation

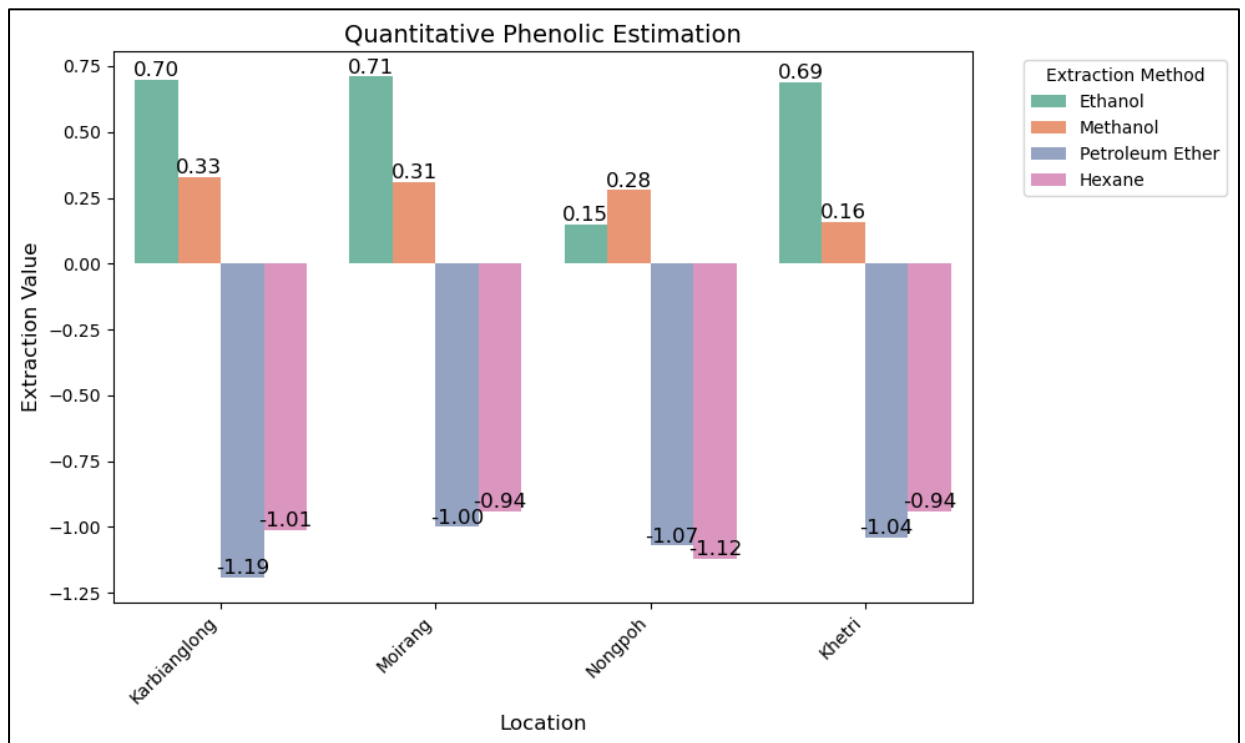


Figure 9: Quantitative Phenolic Estimation

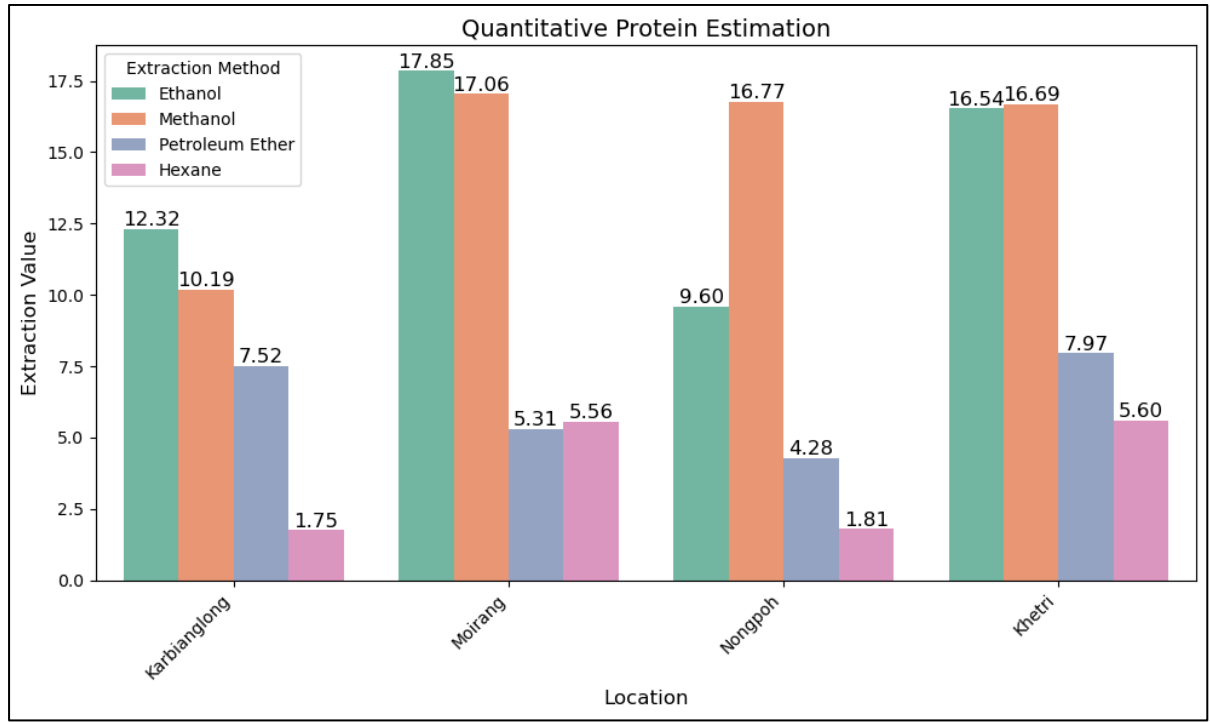


Figure 10 :Quantitative Protein Estimation